

# Digital Fabrication of Pneumatic Actuators with Integrated Sensing by Machine Knitting

Yiyue Luo

yyueluo@mit.edu

MIT CSAIL

Cambridge, Massachusetts, USA

Michael Foshey

mfoshey@csail.mit.edu

MIT CSAIL

Cambridge, Massachusetts, USA

Kui Wu

kwwu@tencent.com

Tencent America

Los Angeles, California, USA

Andrew Spielberg

aespiegelberg@csail.mit.edu

MIT CSAIL

Cambridge, Massachusetts, USA

Daniela Rus

rus@csail.mit.edu

MIT CSAIL

Cambridge, Massachusetts, USA

Tomás Palacios

tpalacios@mit.edu

MIT MTL

Cambridge, Massachusetts, USA

Wojciech Matusik

wojciech@csail.mit.edu

MIT CSAIL

Cambridge, Massachusetts, USA



**Figure 1: Example applications of machine-knitted pneumatic actuators: from left to right, assistive glove, soft hand, interactive robot, and pneumatic quadrupedal robot.**

## ABSTRACT

Soft actuators with integrated sensing have shown utility in a variety of applications such as assistive wearables, robotics, and interactive input devices. Despite their promise, these actuators can be difficult to both design and fabricate. As a solution, we present a workflow for computationally designing and digitally fabricating soft pneumatic actuators *via* a machine knitting process. Machine knitting is attractive as a fabrication process because it is fast, digital (programmable), and provides access to a rich material library of functional yarns for specified mechanical behavior and integrated sensing. Our method uses elastic stitches to construct non-homogeneous knitting structures, which program the bending of actuators when inflated. Our method also integrates pressure and swept frequency capacitive sensing structures using conductive yarns. The entire knitted structure is fabricated automatically in a single machine run. We further provide a computational design

interface for the user to interactively preview actuators' quasi-static shape when authoring elastic stitches. Our sensing-integrated actuators are cost-effective, easy to design, robust to large actuation, and require minimal manual post-processing. We demonstrate five use-cases of our actuators in relevant application settings.

## CCS CONCEPTS

- Human-centered computing → Human computer interaction (HCI);
- Applied computing → Computer-aided manufacturing.

## KEYWORDS

Pneumatic actuators, smart textiles, machine knitting



This work is licensed under a Creative Commons Attribution International 4.0 License.

CHI '22, April 29-May 5, 2022, New Orleans, LA, USA

© 2022 Copyright held by the owner/author(s).

ACM ISBN 978-1-4503-9157-3/22/04.

<https://doi.org/10.1145/3491102.3517577>

## ACM Reference Format:

Yiyue Luo, Kui Wu, Andrew Spielberg, Michael Foshey, Daniela Rus, Tomás Palacios, and Wojciech Matusik. 2022. Digital Fabrication of Pneumatic Actuators with Integrated Sensing by Machine Knitting. In *CHI Conference on Human Factors in Computing Systems (CHI '22)*, April 29-May 5, 2022, New Orleans, LA, USA. ACM, New York, NY, USA, 13 pages. <https://doi.org/10.1145/3491102.3517577>

## 1 INTRODUCTION

Over the last decade, soft actuators have shown enormous promise in applications such as assistive wearables, soft robotics, and interactive devices. In particular, pneumatic actuation is attractive due to its low response time and relatively large output power density. Despite its potential, design and fabrication remains challenging: most common established methods for fabricating soft pneumatic actuators remain slow and manual. Further, incorporating sensorization into such workflows is rarely considered, and simple, established recipes for doing so are lacking.

To overcome the shortcomings of current workflows, we propose a novel method for fabricating pneumatic actuators with integrated sensing *via* machine knitting. Specifically, our method relies on knitting a textile sheath and placing it around an inexpensive, commercial-off-the-shelf elastomeric silicone tube. By programming the extensibility and stiffness of the machine-knitted sheath at stitch level, we can control the actuation response and force the tube to bend, transforming an isotropic and symmetric behavior into one that is directed and can perform useful work. We control the directionality and strength of the tube's bend by strategically placing elastic stitches between normal stitches throughout the knit procedure, thereby controlling the extensibility and stiffness. We also integrate pressure sensing and swept frequency capacitive sensing capability with the actuators *via* a carefully constructed secondary conductive layer.

The choice of knitted actuators affords numerous advantages over traditional workflows: they are machine programmable, allowing for spatially varying materials at the stitch level, which can help to program functionality; they are inexpensive; they are fast to fabricate *via* knitting machines and can be fully knitted and assembled within 5 minutes; and the ability to integrate functional materials allows for a wide array of programmable functionality, such as elastic yarns for elastic mechanical performance and conductive yarns for sensing. Further, knitting, as a long-established, ubiquitous, textile fabrication process, enables the easy incorporation of structures that have been fabricated by other textile-based processes, such as sewing or weaving. Lastly, the textile-based actuator is lightweight and breathable, potentially being useful for a large variety of assistive wearables.

Previous research has demonstrated various attempts for building textile-based pneumatic actuators, such as composing fabrics with different stiffnesses [12, 43], programming textile stiffness with yarn properties and knitting shaping techniques [1, 7], and casting extrinsic reinforcement on textiles [42, 61]. However, most of such constructions still require labor-intensive fabrication cycles, and none of them presents an easy solution for sensing integration. Also, the design process typically requires many iterations without an efficient modeling and simulation tool, which can be tedious and time-consuming. By contrast, our machine knitting process offers programmable and rapid fabrication. Leveraging physically-based simulation techniques, we offer an interactive user interface, allowing users to design and preview actuators' shapes under pressure quickly. After users have finalized their design, the whole knitted structure, including elastic and sensing stitches, is fabricated automatically in one machine run, thus resulting in a complete CAD-CAM pipeline. Our proposed rapid design and fabrication

process boasts a computational yet accessible workflow. Different from previous work, our pipeline boasts a design tool with simulation preview, quick fabrication times, and a digital fabrication process that requires minimal human intervention. We conduct an user-study to evaluate the usability and effectiveness of our computational design interface. We finally demonstrate our system's utility by using it to build assistive wearables, interactive devices, robotic grippers, and locomoting soft robots.

In this paper, we contribute the following:

- A method for rapidly fabricating digitally machine-knitted, customizable pneumatic actuators with integrated pressure and swept frequency capacitive sensing;
- An interactive graphical user interface for design, which allows users to specify and preview actuator behavior easily;
- Characterization of our actuation scheme and evaluation of our actuator's integrated sensing capabilities;
- Demonstrations of our actuator in assistive wearables, interactive input devices, and soft robotics.

## 2 RELATED WORK

In some cases, the work presented in this paper builds upon, and in other cases, stands in sharp contrast to previous efforts. This section describes the landscape of related research in fabricating soft actuators and machine knitting, especially as it relates to smart and functional textiles.

### 2.1 Soft Actuators

Here, we describe previous efforts to fabricate, model, and perform sensing with non-textile-based soft actuators.

*Fabrication.* Several different strategies exist for fabricating soft actuators. Perhaps the most common technique for soft actuation is fluidically-based actuators. Marchese et al. [36] provided several recipes for manufacturing soft, elastomeric, silicone-based actuators, including pneumatic and fluidics. Singh and Krishnan [49] presented a method for further geometrically constraining fluidic actuators to achieve uniaxial behavior. While effective and now in widespread use, these strategies are both manual and require long material casting times. More relevant to our work is the space of *machine-fabricated* actuators. MacCurdy et al. [35] and Wehner et al. [55] presented methods for 3D printing hydraulic actuators that work directly out of the printer; the line of work in Bartlett et al. [8], Drotman et al. [15], Yirmibesoglu et al. [63] presented fabrication methods for 3D printing pneumatic actuators through both inkjet and fused deposition modeling methods. The work in Ma et al. [34] took this one step further and presented methods for computationally designing 3D printed pneumatic actuators with desired deformations. More exotically, actuators based off phase-changes of fluidic material have recently been proposed as a simple, machine-printable actuation scheme [40]. Unlike all of the methods presented above, our actuators are faster to fabricate and easier to integrate with sensing capabilities.

Less widespread strategies for fabricating soft actuators also exist. Dielectric Elastomer Actuators (DEAs) allow for fast response, and it has recently been demonstrated that such actuators can be 3D printed [13, 39]; however, such actuators have low output power-density. The practical inverse of such actuators are liquid crystal

actuators; also 3D printable [31], these actuators have slow response times but high output-power densities. Finally, both bundled nylon-based [59, 62] and shape memory alloys [48] and polymers [18] have recently been demonstrated as actuators for a variety of applications; all such actuation methods can require significant, sometimes impractical bulk to achieve useful response-times and power densities for the applications examined here.

*Sensing.* As silicone and printed rubber are perhaps the most popular medium for housing soft actuators, directly embedding strain sensors as part of a casting process has been a popular way to instrument soft actuators with sensing; see Bächer et al. [6], Homberg et al. [21], Thuruthel et al. [53] for examples. Liquid-metal microchannels can be embedded directly into printing or casting frameworks as well and can provide precise and responsive strain sensing [45, 54], but can require working with toxic materials. Other popular methods for fabricating sensing soft structures include sensorizing foams [51, 52].

## 2.2 Machine-knitted Smart Textiles

Machine-knitted textiles demonstrate attractive features, including softness, flexibility, and conformability. Recent advances in materials development and computational design tools open up the vast potential of digital machine knitting in the field of smart textiles for sensing and actuation applications, especially in the space of assistive technology. We summarize related progress here.

*Machine knitting and design.* In this work, we use an industrial V-bed weft knitting machine consisting of two beds of needles (front and back). Each of the needles can be programmed to perform different needle operations, e.g., knit, tuck, split, and transfer. *Full gauge* indicates knitting every needle, while *half gauge* and *quarter gauge* mean knitting every other needle and every other three needles, respectively. The stitch is the basic element that represents an interlocked yarn loop structure. There are several advantages to using knitting techniques, such as their ability to shape and pattern, e.g., short-rows, increase, and decrease, and for colorwork, e.g., plating and Jacquard knitting. In particular, *short-rows* indicate only knitting partial rows instead of full rows to create local surface extension along the course direction. We refer readers to [38] for more detailed information about machine knitting. Recent developments in computational design tools further facilitate the accessible, interactive, and rapid design processes for digital machine knitting. McCann et al. [38] introduced a compiler that can translate high-level shape primitives into low-level knitting machine instructions in the format of *.Knitout* [37]. Based on a similar idea, Kaspar et al. [28] introduced an interactive web-based design interface based on high-level primitives. In order to provide an editing tool at the stitch level, Yuksel et al. [65] introduced the stitch meshes as an efficient 3D design and modeling interface. The stitch meshes framework was later extended for arbitrary shape conversion [56], hand knitting [57], machine-knitting design [41], and wearable machine-knitting design [58]. Recently, Kaspar et al. [29] introduced a workflow to design and program knitted garments from the traditional cut-and-sew patterns.

*Textile-based actuation.* Fibers in knitted and woven structures have the ability to double as tendon actuators. Textile-based actuation has been especially popular in the space of assistive wearables, where tendon-driven structures have been widely studied [5]. For example, Bern et al. [9] demonstrated a method for tendon-actuating plushies, while Albaugh et al. [3] demonstrated a method to actuate the tendon through knitted structures. Active fibers, such as shape memory alloy fibers [20], strain-programmable fibers [27], and programmable fluidic fibers [30], have also been considered for simplifying actuation.

*Knitted pneumatics.* Pneumatics have also been integrated into textile-based systems as an actuation mechanism. Practically, such bespoke mechanisms have been demonstrated for assistive wearables [12, 17, 43]. McKibben muscles, a specific subclass of pneumatic-driven textiles that rely on a specialized fiber structure to effect muscle-like actuation, have long been analyzed and deployed in robotics [14, 26]. More related to our work, research in the architectural domain has explored knit-constrained pneumatic tubes for actuation [1, 7, 17], which can be deployed more rapidly than the other pneumatic actuators. However, Baranovskaya et al. [7] use a single bed knitting machine, which can only knit planar structures; therefore, the tubular knits covering the pneumatics rely on manual sewing and the stitch transferring require manual intervention. Even though Ahlquist et al. [1] and Elmoughni et al. [17] use a dual bed industrial knitting machine so that the knitting procedure can be automatic, they still need to manually program the knitting patterns without immediate simulation feedback; as a result, multiple design cycles might be required to create desired actuators. More importantly, none of those works provides an automatic way to integrate sensing capabilities. By contrast, our work provides an interactive user design tool which provides users immediate feedback on the actuator shape during editing and converts the design into industrial knitting machine code after users finish the design editing process. Our method also introduces a new knit architecture that features integrated sensing, unlocking applications in assistive and robotic devices.

*Textile-based sensing and human-computer interaction.* Thanks to recent innovations in advanced materials, design, and fabrication techniques, diverse sensing capabilities such as inductive [19], capacitive [47, 60], and resistive sensing [2, 46], have been integrated into textiles, leading to applications such as interactive input devices [24, 33, 44] and sensing wearables [25, 32]. Similar to some previous work, our sensing architectures integrate conductive yarn through machine knitting. Contrasted with that line of work, the new sensing structure we propose is capable of robust sensing even in the presence of large actuation-based deformation.

## 3 METHOD

Our sensing-integrated pneumatic actuators are computationally designed and digitally fabricated using a V-bed knitting machine (SWG091N2, Shima Seiki). By using both the front and back needle beds, we are able to generate tubular knits. In this section, we describe our actuation and sensing principles in detail.

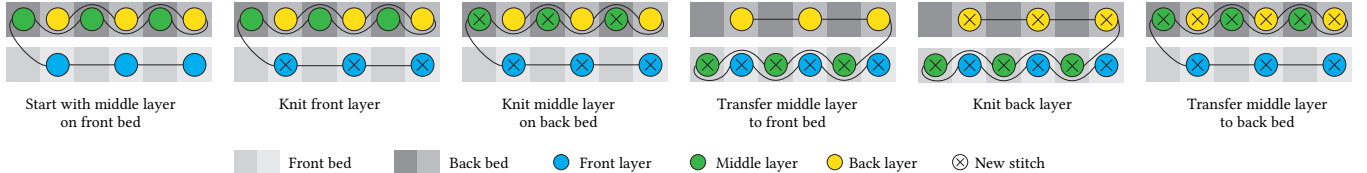


**Figure 2: Illustration of three-layered structure knitting: our three-layered knitting structure is enabled by the recurrent transferring of the middle layer between the front and back bed.**

### 3.1 Actuation Principle

Our actuator is composed of two parts: an off-the-shelf thin-wall silicone tube, which serves as the base pneumatic channel, and the knitted sheath with programmed stitches, which wraps over the silicone tube and confines the shape of the inflated actuator. The deformation of the actuators is mainly defined by the knitted sheath with locally variable extensibility. We manipulate the extensibility of the knits with two parameters: stitch densities and stitch types. Using only one of every two or four needles on the knitting machines, we can generate half gauge or quarter gauge knits with higher flexibility and extensibility. Moreover, varying stitch types offers distinction in mechanical performance. In particular, we use an elastic yarn (Lycra, Uppingham Yarns), which is about 100 times more extensible than acrylic yarn. An elastic feed device enables the knitting of elastic yarn, which pre-stretches the elastic yarn and controls its advancement using a stepping motor. To stabilize the knitting process and maintain the straight tubular configurations of the knitted sheath, we integrate the elastic yarns in the form of short-rows, which are only knitted locally at selective locations. Some examples of our support stitch patterns can be seen in Fig. 7 (top). The scale of actuators presented in this paper is dictated by the size and wall-thicknesses of presently-available commercial silicone tubes; however, the principle beyond our actuator's design is scale-agnostic.

As an example, an actuator design is demonstrated in Fig. 3. The front of the tubular knits is constructed with normal acrylic knitting yarn (normal stitches), and the back of the tubular knits is

constructed with a mixture of normal stitches and elastic stitches. More specifically, the elastic stitches are composed of knits with normal acrylic yarn and short-rows with elastic yarn. We then wrap the knitted sheath over the silicone tube and anchor both ends of the wrapped tube with clamps. When the silicone tube is inflated, the elastic stitches at the backside tend to extend more than the non-elastic stitches, forcing the tube to bend to another side. It is noted that the knitted sheath maintains a straight tubular shape before the actuator is inflated, as shown in Fig. 3 left. This is a consequence of the design: the short-rows of elastic yarn tend to shrink once released from the machine, and both the front and back sides obtain the same number of knitting courses by acrylic yarn. By placing the normal stitches and elastic stitches at designed locations, we can program the shape of the inflated actuators.

In this paper, we demonstrate our actuation principle on assistive wearables and grippers, which may have multiple actuators each requiring a single degree of freedom; but, further, we also demonstrate a soft locomoting robot whose motion requires actuators with multiple degrees of freedom. To this end, we design and fabricate a three-layered knitted structure, which can hold a pair of actuators to enable the structure to bend along both forward and backward directions. In particular, the front and back layers are composed of elastic stitches. The middle layer is composed of normal stitches and shared by both silicone tubes. Since we use a v-bed knitting machine with two needle-beds, front and back, a special treatment is needed to knit the three-layered structure. To be more specific, the stitches in the middle layer are recurrent transferred between the front and back beds. For example, in each knitting cycle, we first knit the back layer on the back bed while temporally holding both the front and middle layers on different sets of needles (half gauge) in the front bed. Then, we knit the middle layer on the front bed and transfer it to the back bed (Fig. 2). Lastly, we knit the front layer, transfer the middle layer back to the front bed, and start a new cycle. We repeat this knitting cycle until we have the full sheath.

### 3.2 Sensor Designs

We integrate two different sensing capabilities to our machine-knitted pneumatic actuators: resistive pressure sensing and swept frequency capacitive sensing. Both sensing capabilities are enabled by the usage of standard off-the-shelf conductive yarns (80% polyester and 20% stainless steel). We optimize the design so that our resistive and capacitive sensors are not affected by the inflation and bending of the actuators.

**3.2.1 Resistive pressure sensing.** We leverage the plating technique to insert conductive yarns at specific locations. Specifically, the

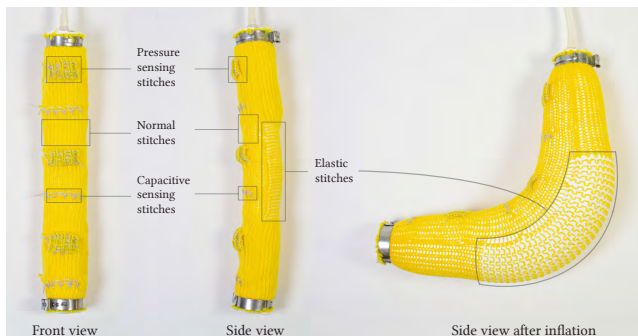


**Figure 3: Overview of a machine-knitted sensing-integrated actuator: three spaced pressure sensors and three spaced electrodes for swept frequency capacitive sensing are located at the front of the knitted sheath; the elastic stitches at selective locations in the back of the knitted sheath enable the bending of the actuator.**

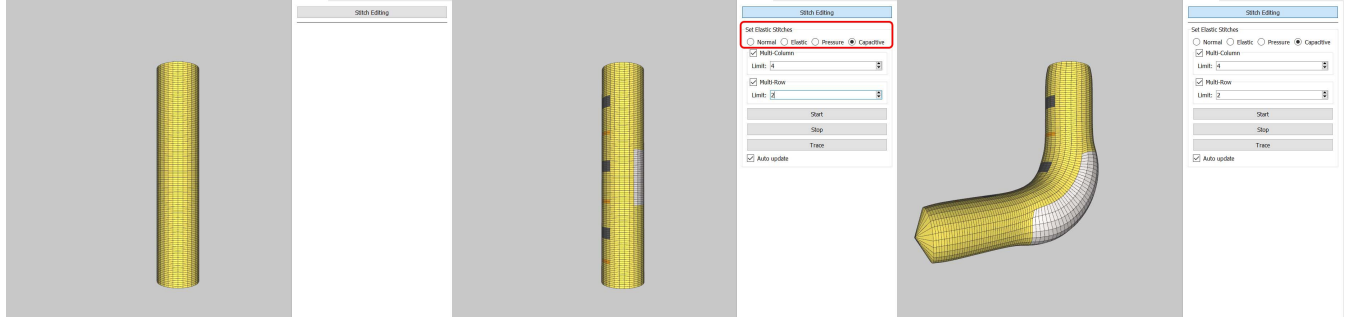


**Figure 4:** Our interactive design interface: left, the user starts with a sketch tube, which is a simple tubular knit structure with all normal stitches; middle, the user paints the tube with different stitch types highlighted in red; right, the predicted (actuated) actuator shape based on user’s design. ■, □, ■, and ■ indicate normal, elastic, pressure sensing, and capacitive sensing stitches, respectively.

conductive yarns are blended with normal acrylic knitting yarn *via* a pressure sensing stitch. The knitted conductive yarn loops interlock loosely when there is no external pressure. The conductive loops collapse when applying a load, resulting in more electrical paths; thus, the resistance drops. The sensor measurements are amplified and converted to a digital signal by a read-out circuit.

One of the biggest challenges is to make the pressure sensor insensitive to actuator-driven expansion. Since the resistive pressure sensors share the same base knitted substrate with the pneumatic actuators, previous knitted sensor designs, like [33], cannot provide reliable pressure sensing when the actuator is inflated, stretching the pressure sensor and collapsing the conductive loops. To this end, we propose a new pressure sensor design with a few special treatments. First, by splitting and transferring the existing yarn loops, we construct the pressure sensing stitches on a separate layer on the stiffer side of the actuator. Moreover, as shown in Fig. 3, we design the pressure sensor with lower stitch density and larger local curvatures by using quarter gauge and short-rows. Therefore, our pressure sensor obtains minimal connections with the base knitting substrate and additional flexibility and surface area compared with the base knitting structure. As a result, our design prevents the pressure sensors from being stretched when the actuators activate and ensures the reliability of pressure sensor performance.

**3.2.2 Swept frequency capacitive sensing.** Swept frequency capacitive sensing leverages the fact that alternating current (AC) signals of different frequencies flow through different paths at the capacitive interface between the electrode and body-contacted objects [22, 47]. By collecting amplitude responses over a range of frequencies, we retrieve information on the existence of human touch or human-contacted objects. We generate square wave sweeps from 100 kHz to 1.6 MHz in 5 kHz steps (300 steps in each sweep) and transform them to sinusoidal waves using an LC (inductor-capacitor) oscillator. We measure the return voltage signal over a 1 M $\Omega$  resistor. We use an Adafruit Metro M4 (ATSAMD51) for signal processing.

Like the integrated pressure sensor, we use a separated layer to construct the electrode for swept frequency capacitive sensing, but we knit the capacitive sensing stitch with conductive yarn only

instead of plating normal and conductive yarns. We separate capacitive sensing stitches and pressure sensing stitches with at least two courses of normal stitches to prevent shorting among the integrated conductive yarns and reduce interference. To aid readers in better understanding our knitted structure, we also include a sample .knitout code in the supplemental material. This code enables knitting of the actuator (Fig. 3) with pressure and capacitive sensors using the V-bed knitting machine (SWG091N2, Shima Seiki) as well as visualization through an online knitout visualization tool.<sup>1</sup>

## 4 INTERACTIVE DESIGN PIPELINE

To allow users to design and preview inflated actuators quickly, we provide an interactive design system by which users are free to specify the locations of elastic stitches, pressure sensors, and capacitive sensors. Our system can then convert the user’s design into low-level machine instructions for immediate digital fabrication.

### 4.1 Design Interface

Our design interface is built on quad Stitch Meshes [33], where each stitch structure is abstracted as a quad mesh face. Users mark each face with one of four stitch types. The *normal stitch* ■ is knitted with standard acrylic yarn as the base structure. Our actuation programming principle is based on inserting short-rows (additional partial rows in the middle of other full rows) that are fully knitted using elastic yarns. However, inserting a short-row would require modifying the mesh topology. To preserve the same mesh topology during stitch type authoring, we use the *elastic stitch* □ to represent one normal stitch and two elastic stitches next to each other along the elongated direction. Both the *pressure sensing stitch* ■ and the *capacitive sensing stitch* ■ represent double-layered structures where the front layer is knitted with conductive yarn. As shown in Fig. 4 (left), the user starts by generating a tube by inputting a specific number of rows and columns. Each quad represents one stitch and is marked as a normal stitch by default. Then, the user can design the actuator by labeling individual faces or sets of faces with the desired stitches (Fig. 4 middle).

<sup>1</sup><https://textiles-lab.github.io/knitout-live-visualizer/>

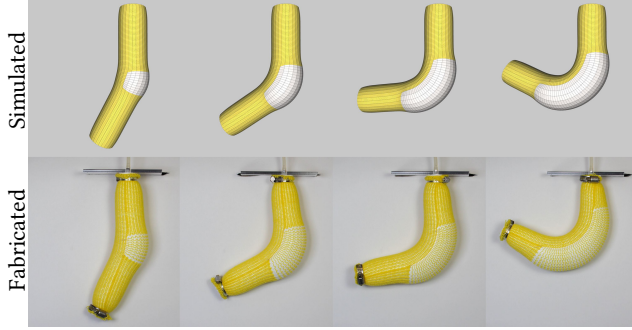


**Figure 5: Comparison between simulated and fabricated actuator shapes with different number of elastic rows at same air pressure: top, predicted results from our simulator; bottom, fabricated results. From left to right, 10, 20, 30, and 40 rows of elastic stitches. Yellow faces ■ are normal stitches and white faces □ are elastic stitches.**

## 4.2 Predictive Simulation

Our system also provides an interactive preview of the actuator's shape when the user adds or removes elastic stitches (Fig. 4 right). To achieve this, we deploy a physically-based simulation to minimize the potential energy  $E(\mathbf{x})$  when the physical system is at equilibrium under pressurization, meaning sum of the internal force  $\mathbf{f}_{\text{int}}$  and the pressure force  $\mathbf{f}_{\text{pressure}}$  should be zero at any point on the actuator's surface. We can formulate the equilibrium problem as solving for  $\mathbf{x}$  such that

$$\mathbf{f}_{\text{pressure}}(\mathbf{x}) - \sum_i w_i \nabla E_i(\mathbf{x}) = \mathbf{0} \quad (1)$$

where  $\mathbf{x}$  is a vector corresponding to the vertex positions in the quad mesh state, and  $E_i$  is defined as three different types of constraints based on our observation of knit behaviors.

First, we use a rectangle constraint to enforce each face to be rectangular since the course edges and wales edges are typically perpendicular to each other for a *knit* stitch. To solve this, we first project the corners of the quad face onto their least-squares plane and then fit the rectangle in 2D as mentioned in [10]. The anisotropic deforming behavior for each knit face is modeled as distance constraints with different stiffnesses for wales edges and course edges, respectively. Thirdly, bending constraints are added to the adjacent quads to minimize the difference between the mean curvature of the deformed and undeformed quad surface [11]. Like [50], The pressure force on each quad is defined as

$$\mathbf{f}_{\text{pressure}}(\mathbf{x}) = A(\mathbf{x})P\mathbf{n}, \quad (2)$$

where  $P$  is the pressure value,  $\mathbf{n}$  is the outward face normal, and  $A(\mathbf{x})$  is the quad area that depends on node position  $\mathbf{x}$ . To solve Eq. 1, we use Projective Dynamics [11], which uses a pre-factorized system matrix to achieve the interactive frame rate for the simulation.

To obtain a realistic simulation result, we use a data-driven strategy to capture the shape of individual normal and elastic stitch faces under pressure. In particular, we first inflated two actuators: one with all normal stitches and one with all elastic stitches. Then, we measured the length and radius of those two actuators, respectively, and converted them to the width  $w$  and height  $h$  of the individual face. During simulation, we use  $w$  and  $h$  as the rest width and height

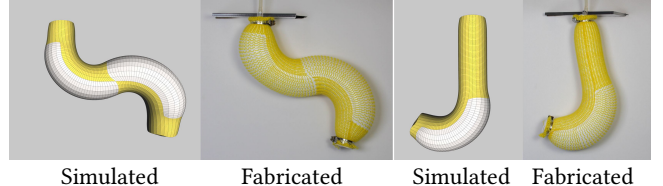


**Figure 6: Qualitative design results: "S" and "J" shapes designed using our tool.**

for each quad. To verify our result, we fabricated four actuators with 120 rows and 28 stitches per row as shown in Fig. 5. Under 500 mbar, our predicted results are qualitatively similar to the physical experimental results for the actuators with 10, 20, 30, and 40 elastic short-rows.

## 4.3 Knitting Instructions Generation

Since we insert a silicone tube with a uniform radius inside the knitted sheath, we only consider tubular knitted structures with the same number of stitches every row. From this constraint, it is straightforward to trace the knitting patch from the bottom to the top and schedule the needle location for each face. To generate the machine instructions, we first pre-trace the current row to check if sensor stitches exist. If so, we split the stitches at sensor stitch locations and merge them back after knitting the sensors. The elastic stitches can be added easily by knitting additional short-rows at elastic stitch locations after finishing the current row. Fig. 6 shows two examples of actuators designed using our system. More details can be found in the supplemental video.

## 5 CHARACTERIZATION

In this section, we perform diverse characterization experiments to quantitatively evaluate the performance of our actuators, integrated resistive sensors, and capacitive sensors. We control the activation of our actuators by a pneumatic control system (Festo), which is consisted of 16 individual valves for independent control of 16 actuators. Actuators are controlled by commanding manually-specified target pressure sequences; these pressures are achieved and maintained by PID controllers embedded on valve hardware. This control scheme is used for all examples in this paper, except for pressures commanded in "response" to sensed stimuli (responses are still pre-programmed, but they are not commanded as fixed open-loop sequences).

### 5.1 Actuator

The ability of our actuator to reach desired deformations relies on the extensibility variation enabled by knit structures and stitch types. Therefore, we first perform tensile testings (Shimadzu AGS-X) on knitted fabrics (3 cm × 6 cm) with different normal stitch densities and elastic short-row density. Generally, compared with knits with low stitch density (quarter gauge, Young's modulus of 0.18 GPa and tensile strength of 0.24 GPa), knits with higher stitch density (half gauge or full gauge) demonstrate higher Young's modulus (0.22 GPa for half gauge 0.54 GPa for full gauge) and tensile strength (0.44 GPa for half gauge 1.29 GPa for full gauge). Moreover, since the elastic yarn is more extensible than the acrylic knitting

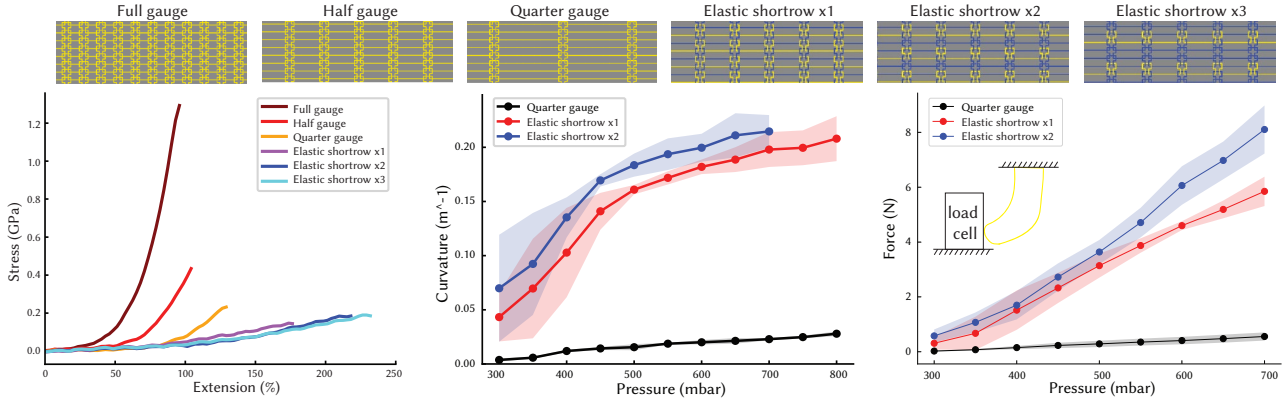


**Figure 7: Actuator characterization:** top, illustrations of different knitting structures (normal yarn in yellow, elastic yarn in blue) (visualizing in the web-based UI [64]); left, stress-strain characteristics of knits with different structures; middle, curvature of pressurized actuators with different knitting structures; right, exerted force of pressurized actuators with different knitting structures (measurement set-up illustrated in the sub-plot). Characterization is done on three different samples.

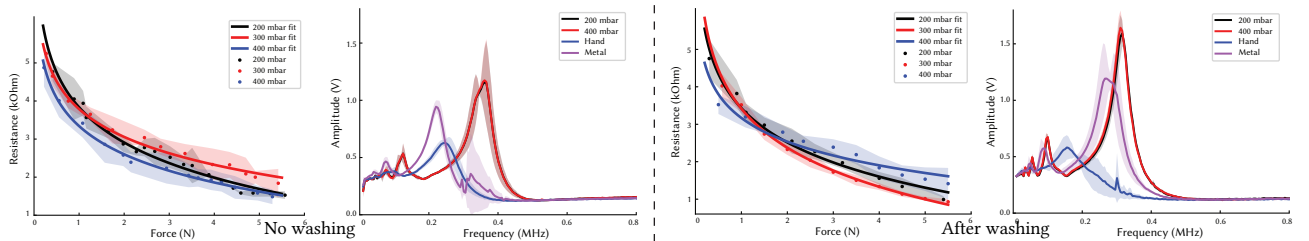


**Figure 8: Sensor characterization:** left, resistance profile of the integrated pressure sensor under load and representative amplitude responses from swept frequency capacitive sensing; right, our pressure and capacitive sensors obtain similar performance after a regular washing and drying cycle. All characterizations are performed on three samples.

yarn, given the same stitch density (half gauge), knits with the higher compositions of elastic yarn demonstrate lower Young's modulus (as low as 0.18 GPa) and higher elongation (up to 230 %), as shown in Fig. 7.

We fabricate multiple knitted sheaths to characterize the bending performance of actuators that are composed of different sets of knitting structures. In particular, the front is always composed of half gauge normal stitches, and the back is composed of either quarter gauge normal stitches or half gauge elastic stitches with different densities (one or two elastic short-rows). We then wrap them around silicone tubes (1.5 mm in thickness) and assemble them into actuators (2 cm in diameter and 16 cm in length). We measure the bending radius (curvature) when the actuators are activated up to 800 mbar (Fig. 7). We further measure the forces exerted by the actuator at the tip. We measure the response from the fixed load cell when the actuators are activated. The testing setup is shown in the inset figure. Our actuators can bend with curvatures up to  $0.2 \text{ m}^{-1}$  and exert forces up to 9 N at the tip, which is comparable to previous work in fabric-based pneumatic actuators [12].

To prevent breakage, we need to keep the extension of the knitted fabric below its yield strain. Both normal knits and elastic knits are strong enough to endure the expansion even with more than 100%

of extension, which is much higher than the experienced stretch of our actuators at this stage. We also performed 100 cycles of an inflate/deflate test with air pressure at 700 mbar, the maximum pressure we used for our applications. We observe the actuator obtains stable performance without any breakage of yarn.

## 5.2 Sensing

Our typical pressure sensor is about  $2 \text{ cm} \times 1 \text{ cm}$ , realized as  $5 \times 12$  stitches in quarter gauge. We characterize the performance of our pressure sensors by measuring resistance (DMM 4050, Tektronix) while applying loads up to 5.5 N at various actuator pressurization. A typical sensor's resistance drops when the applied load increases from 1.5 N to 5 N. As shown in Fig. 8 left, the resistance profile of our pressure sensor is barely affected by the activated pressure, which demonstrates the ability of our knitted structure design to operate accurately under a wide range of actuation.

Fig. 8 left shows the characteristic amplitude responses from the swept frequency capacitive sensing. The black and red curves almost coincide, indicating that the actuating pressure similarly does not affect the swept frequency capacitive sensing performance. On the other hand, the amplitude responses, in terms of the peak position and magnitude, vary significantly when the electrode is in

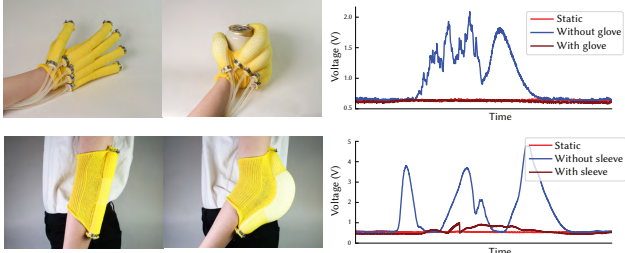


**Figure 9:** Assistive wearables: top, the activated assistive glove facilitates the grasping of a filled can with minimal muscle activities; bottom, the assistive sleeve facilitates the bending of the elbow.

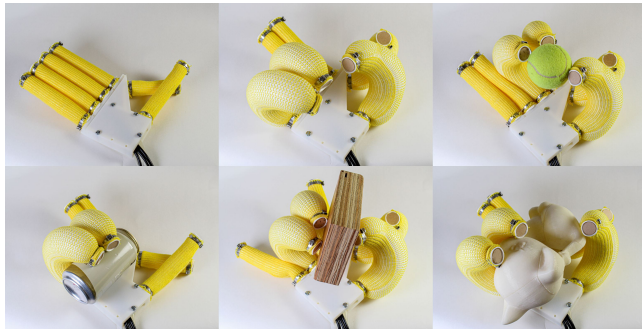


**Figure 10:** Soft hand: the actuation of each finger is individually addressable by a pneumatic valve system, allowing us to realize a variety of hand poses and grasp objects with different shapes, textures, and weights.

contact with the human body or human-contacted conductive substrate, making this sensing modality useful for human interaction.

We further perform a washing test to verify the reliability of our sensors. We measure the performance of our pressure and capacitive sensors after a regular warm washing and medium drying cycle. As demonstrated in Fig. 8 right, the performance of both sensors after the washing cycle is very similar to that without washing.

## 6 APPLICATIONS

This section demonstrates our actuators in a diverse set of application scenarios in assistive wearables and soft robotics. We demonstrate both our actuation and sensing capabilities and showcase some examples that require both.

### 6.1 Assistive Wearables

Soft actuated wearables serve as attractive solutions for assistance in medical and health applications. Our machine-knitted pneumatic actuators have outsized potential as assistive wearable solutions because they are low-cost, lightweight, breathable, conformal to the human body, and compatible with the current garment manufacturing processes. We demonstrate our actuators' potential and capability in wearable devices by seamlessly integrating them into knitted garments such as gloves and sleeves. An assistive glove with 5 actuators on the top surface of each finger is demonstrated in

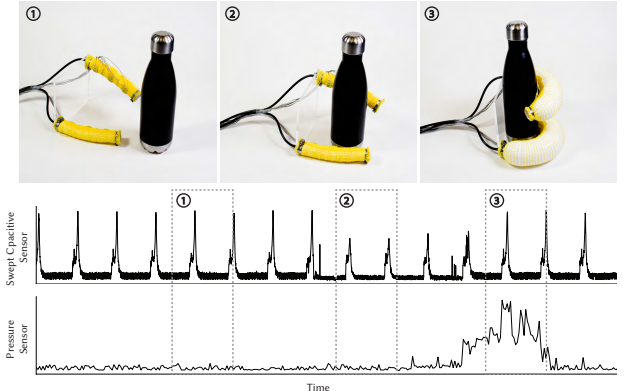


**Figure 11:** Two-finger gripper: a typical grasp sequence of the two-finger gripper alongside the average recorded signal of the 6 integrated pressure sensors and the recorded amplitude response from the capacitive sensor.



**Figure 12:** Interactive actuator: the integrated swept frequency capacitive sensing detects human's touch and the actuators activate with shape changes.

Fig. 9. The whole glove is knitted in one machine run. Each actuator is designed to enable the forward bending motion, which facilitates the corresponding finger flexion. The assistive glove enables geometrically and materially diverse objects to be grasped securely within approximately 1.5 seconds. We also designed and fabricated a shirt sleeve with actuators that can assist in elbow bending. We demonstrate the utility of our assistive wearables by comparing electrical activities of muscles under different circumstances, which are measured by placing an electromyography (EMG) sensor (Advanced Technologies) at the extensor digitorum communis (EDC) muscles. Minimal muscle activities are observed while completing tasks and motions when using the assistive glove and assistive sleeve, as shown in Fig. 9 (plots on the right).

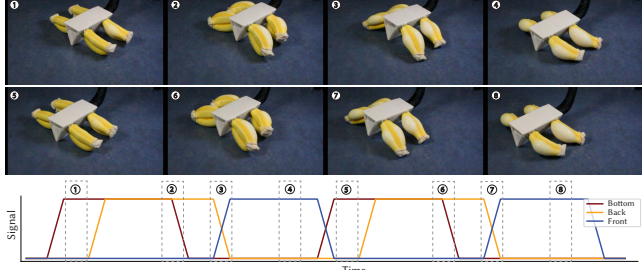
### 6.2 Soft Hand

We design and fabricate a soft hand with six individual machine-knitted actuators. We specifically incorporate two actuators for the thumb to mimic the utility of human thumb opposability. The actuators are mounted on a 3D printed palm-shaped holder. As demonstrated in Fig. 10, by activating different sets of actuators, we can perform diverse grasps on objects of various sizes, geometries, and weights, from a tennis ball to a wooden block, in a reliable manner.

### 6.3 Sensorized Gripper

We demonstrate a two-finger gripper with integrated pressure sensors and swept frequency capacitive sensing. We integrate three

Example	Assistive glove	Assistive sleeve	Soft hand	Two-finger gripper	Interactive robot	Quadrupedal robot
Knitting time	35 min	8 min	15 min	14 min	14 min	45 min
Assembly time	8 min	2 min	15 min	6 min	8 min	30 min

**Table 1: Fabrication and assembly time for each example****Figure 13: Quadrupedal robot walking forward: status of the robot walking forward at different stages of the leg actuation sequence.**

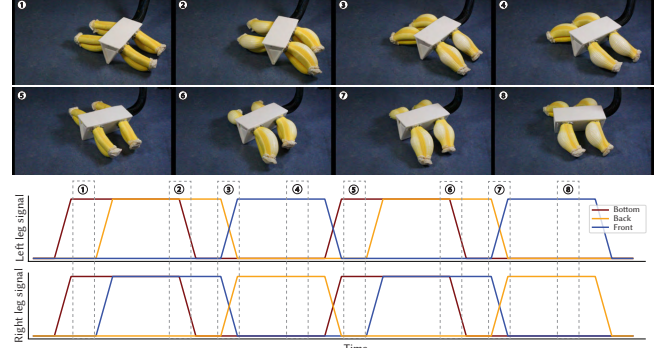
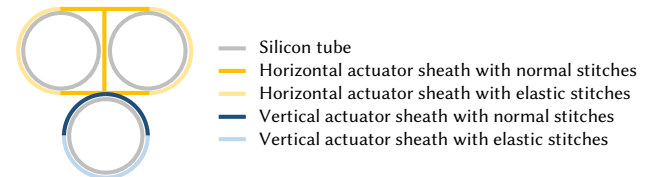
pressure sensors and two electrodes for swept frequency capacitive sensing on each finger. The amplitude response from swept frequency capacitive sensing offers real-time feedback on the presence of objects along with the finger interior. The integrated pressure sensors provide real-time feedback on the quality of the grasp. Fig. 11 presents a montage of a typical grasp procedure. First, the pressure and capacitive sensors exhibit the default response when the gripper is not yet in contact with the object. Second, the gripper establishes loose contact with the water bottle, whose conductive bottom induces a change in the capacitive signal. The pressure sensors exhibit no response at this stage. Lastly, the actuators are activated to power grasp the object once the object is detected. The signal from the pressure sensors increases, corresponding to the rise of force between the actuators and the object. Once the pressure sensor reading exceeds a threshold, the grasp is registered as successful. The success of the grasp is confirmed by lifting and shaking the gripper while maintaining the stability of the grasped object; more details can be found in the supplementary video.

#### 6.4 Interactive Actuators

Our machine-knitted actuator with integrated swept frequency capacitive sensing can be used as an interactive robot. We assemble four separate actuators, each integrated with an electrode for the swept frequency capacitive sensing. Real-time sensing feedback allows the robot to respond interactively: when a human's touch is detected with an actuator, they either activate (if inactive) or deactivate (if active).

#### 6.5 Pneumatic Robot

Our machine-knitted pneumatic actuators can further be arranged as legs for a soft quadrupedal robot (Fig. 13). Each of the four legs consists of three actuators, two of which antagonistically bend in the lateral direction (forward and backward) while the third turns the leg upward vertically. We note that it is hard to knit multiple layers in the V-shape knitting machine. As a solution (Fig. 15), we design and knit each of the four legs in two machine runs: one run to fabricate a pair of horizontal actuators as mentioned in Sec. 3.1

**Figure 14: Quadrupedal robot turning: robot turns to right by actuating legs on the left forward and legs on the right backward.****Figure 15: Cross-section view of a typical robotic leg design**

and the other to fabricate the vertical actuator. Then, the vertical actuator is sewed and affixed to the pair of horizontal actuators. The horizontal actuators are designed and manufactured explicitly as a pair in one run to reinforce each other's motion relative motions, and their movements in the vertical direction are minimized.

We pre-define the motion pattern of each leg, which includes four steps that combine to form a rowing-like motion. First, the actuator at the bottom bends upward to lift the leg off the ground. Then the horizontal actuators turn forward. After that, the bottom actuator releases to put the leg down. Finally, the horizontal actuators bend backward, achieved by releasing the activated actuator and activating the resting one. This final motion pushes the robot forward, while the preceding three ready the actuator into position. To increase the friction between the robot and the floor and facilitate the pushing motion, we wrap a latex membrane over the tips of the quadrupedal robot legs. As demonstrated in Fig. 13, the quadrupedal robot can locomote forward and backward by actuating all legs with the same sequence. The robot can further achieve a turning motion by actuating the legs on one side forward and the other side backward.

In summary, we highlight that our design and fabrication pipeline is fully digital. Typically, the user only needs to spend a few minutes customizing and finalizing the actuation design. Then, the designs are knitted automatically in an industrial knitting machine. We record the knitting and assembly time in Table 1, which shows

that our proposed machine-knitted pneumatic actuator system is easy and fast to fabricate and assemble.

## 7 USER STUDY

We conducted an experiment to evaluate the usability and effectiveness of our computational design interface. Our goal is to investigate whether our design interface, which incorporates predictive simulation, improves design efficiency.

### 7.1 Procedure

Eleven participants (3 female) between 21 and 30 participated in the study. We first provided participants with a tutorial of our design user interface. We then let users design a simple “S” shape actuator with the feedback from the predictive simulation to ensure they were familiar with the interface. Next, we asked participants to perform two tasks that have been widely used for evaluating soft robot design [4, 16, 23]. The first task asked users to design an actuator such that the endpoint of the actuator would make contact with a specified location (red dot) when inflated. The second task asked users to design an actuator that can circumnavigate a specified obstacle (gray cylinder) *while* hitting the target (red dot) when inflated. The task setups are shown in Fig. 16. During the study, we first asked all participants to perform those tasks without simulator feedback. Users were not informed on the actuated shape of their designs during or after designing. Those designs were used as our baseline. Then, we asked all participants to perform the same tasks again with the predictive simulation enabled, which offers intermediate feedback during the design process. We used the output designs as the experimental group.

To quantitatively and qualitatively measure the usability and effectiveness of our method, we define four metrics, *time*, *accuracy*, *difficulty*, and *confidence*, in which the first two are objective, and the latter two are subjective. Our method has high *usability* if participants can design actuators with high accuracy while using a small amount of time. Our method has high *effectiveness* if the participants believe the tool is easy to use and feel confident in their designs. We tracked the amount of time participants spent on each task and measured the accuracy of participants’ designs by calculating the distance  $D$  between the end of the actuator and the

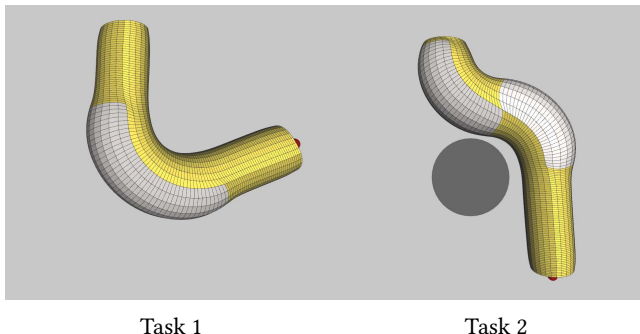


**Figure 16: Task setups:** left, task 1 asked users to design an actuator whose end would hit the target (red dot) when actuated; right, task 2 asked users to design an actuator that would hit the target (red dot) and avoid the obstacle (gray cylinder).

target and the overlapping distance  $O$  between the actuator and the obstacle. After the study, participants filled out a post-experiment questionnaire, where they indicated subjective ratings for the difficulty of each task (with and without predictive simulation), as well as the confidence of whether the fabricated designs would behave as desired using a continuous numerical scale.

### 7.2 Results

All participants indicated a positive experience ( $4.73 \pm 0.47$  given the scale from 1 to 5, where 1 is the worst and 5 is best). The design time and accuracy on each task, as well as participants’ subjective ratings on task difficulty and confidence on designs, are demonstrated in Fig. 17. We also fabricated six randomly selected participant designs as examples and compared them with our simulation results. The fabricated and simulated results are shown in Fig. 18. In general, participants achieved higher accuracy in both tasks, considered the tasks easier, and obtained more confidence in their design when our predictive simulation tool was provided. Such results indicate the usability and effectiveness of our design pipeline.

*Design time.* Participants finished the designs within 2 minutes on average without the predictive simulation and within 5 minutes when given the simulation. Participants generally spent more time on designing when the predictive simulation was included in the pipeline, which is expected as we observed that our tool with predictive simulation offered participants an opportunity to iterate on and improve their designs.

*Design accuracy.* All designs are 19 cm long with the radius of 2 cm without inflation. Assuming the axis and radius of the cylindrical obstacle are  $L$  and  $R$  ( $R = 2.83$  cm), we computed  $O$  as  $R$  minus the closest distance between the actuator and the axis  $L$ . Ideally, we expected  $D$  is close to zero, indicating hitting the target, and  $O$  is smaller or equal to zero, indicating no collision between the actuator and obstacle. As demonstrated in Fig. 17 middle left, when offered our predictive simulation pipeline, participants were able to create designs with higher end-effector accuracy. Most actuators designed while using simulator feedback could reach within 5cm of the target. Furthermore, all participants could create designs that bypassed the obstacle when using our predictive simulator, which wasn’t always true when the simulation was disabled. Although participants spent more time designing when relying on simulator feedback, the resulting designs were expected to be much more effective.

*Difficulty.* Regarding the difficulty, participants gave  $4.17 \pm 0.75$  for task 1 and  $4.67 \pm 0.82$  for task 2 when predictive simulation was disabled, which indicates that participants found both tasks very difficult without the predictive simulation. Here, the score range is from 1 to 5, where 1 represents the easiest and 5 represents the most difficult). In contrast, when the predictive simulation was offered, the difficulty score decreased to  $1.5 \pm 0.83$  and  $1.83 \pm 0.75$  for task 1 and task 2, respectively. We can conclude that those participants found the tasks significantly easier when predictive simulation is available.

*Confidence.* When designing with the predictive simulation, participants were very confident that the fabricated actuator would behave as desired ( $4.73 \pm 0.47$  for task 1 and  $4.64 \pm 0.50$  with the scale

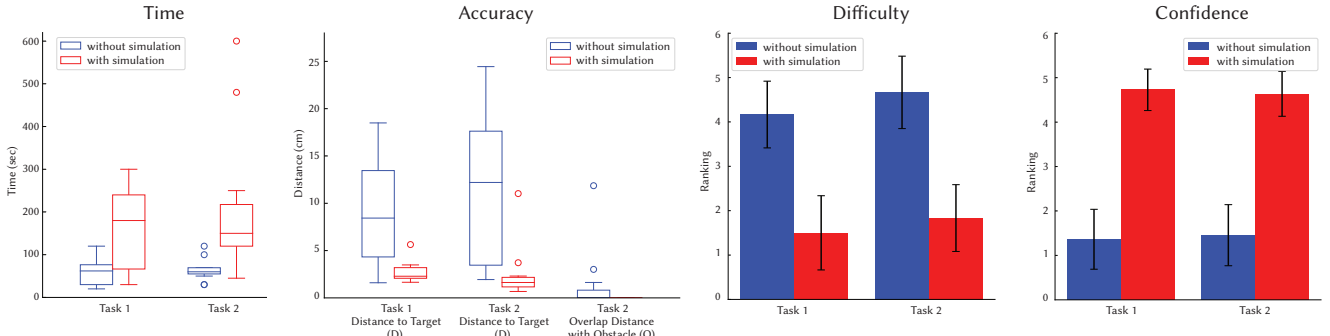


**Figure 17: User study results: left, design time for each task; middle left, quantitative design accuracy; middle right, subjective rating of difficulty of each task (scale 1 to 5, where 1 represents the easiest and 5 represents the most difficult); right, subjective rating of confidence on the designs (scale 1 to 5, where 1 represents the least confidence and 5 represents the highest confidence).**

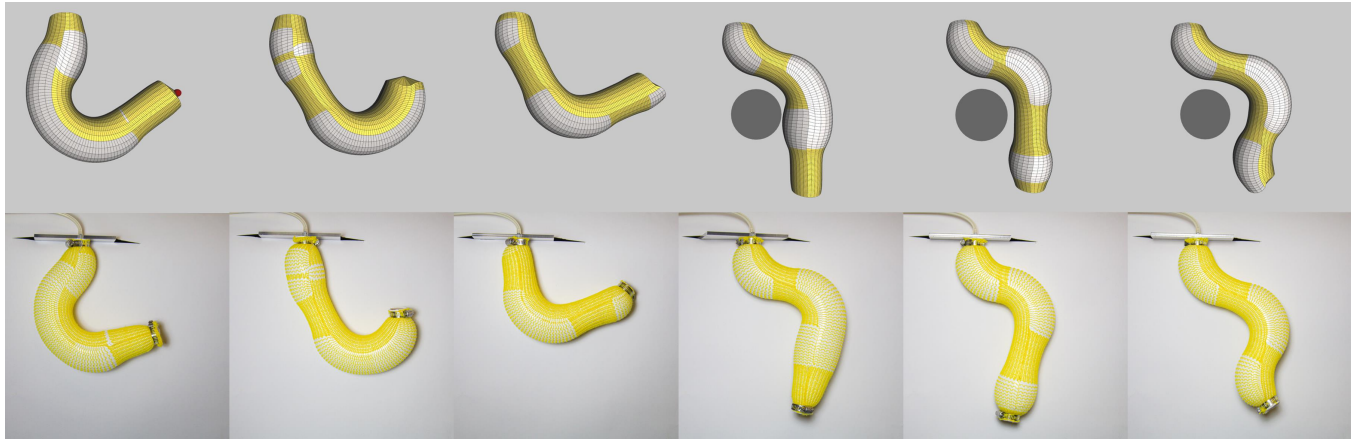


**Figure 18: Example designs by participants: top, participants' designs in our design pipeline with predictive simulation; bottom, the corresponding fabricated actuators.**

from 1 to 5, where 1 represents the least confidence and 5 represents the most confidence). In contrast, participants were generally not confident with their designs without the predictive simulation ( $1.36 \pm 0.67$  for task 1 and  $1.45 \pm 0.69$ ). We further validate our predictive simulation by fabricating three randomly selected designs from each task. Fig. 18 demonstrates the fabricated actuators obtain quantitatively similar behavior as the simulated prediction.

## 8 LIMITATIONS AND FUTURE WORK

*Complex actuator/sensing design.* Currently, it is challenging to incorporate our sensors over the entire body of the actuator, given the extensive stretching of the elastic yarn. Also, our V-bed knitting machine only allows for fabricating actuators with bending motion along one specific direction at a time, which limits the actuators' degrees of freedom. For the quadruped example in Fig. 13, separated knitting processes and manual sewing post-processing steps are needed to make the leg bend into multiple directions. Further, we would like to extend our design tool to incorporate task-driven, optimization-based design, where users specify target poses and optimal stitch patterns can be synthesized automatically.

*Actuators of diverse shapes and sizes.* As demonstrated by recent work [41, 58], machine knitting is compatible with complex 3D geometry. The same principle of actuation and sensing can be extended to any geometries and size as long as the corresponding pneumatic channels are available. For ease of rapid fabrication, in our experiments, we use only one type of thin-walled commercial off-the-shelf silicone tubes. However, if commercial thin-walled silicone bladders of other shapes and sizes were made available, our method should be directly applicable for actuators with diverse shapes, sizes, and bending performance, opening up new potential applications. It would be worthwhile to verify this in future work.

*The granularity of actuation.* The bending performance of the actuator is determined by the knitted sheath designs as well as pneumatic channel properties, e.g., wall thickness, radius, and materials. Those parameters and the air pressure level further determine the overall volume of inflated actuators. Our predictive simulation model is guided by the experimental results of inflated actuators using only one type of thin-walled silicone tube. It would be interesting to build an automatic system identification pipeline for

actuators with different pneumatic channels and elastic yarns in the future.

*Sensing.* As one limitation, during grasping, we notice that direct contact with grasped objects mostly occurs at the fingertips, which limits the utility of our integrated sensors distributed throughout the actuators. As a salient avenue for future work, it would be very useful to develop strain sensing capability, which would offer proprioception information for the actuators and robots. It would be interesting to explore knit architectures that could provide more spatially-rich contact information; approaches (e.g., [25]) that combine learning with sensor data could be helpful here. Furthermore, coupling the sensing capabilities of our actuators with modern machine learning techniques could enable diverse cognitive robotics tasks such as grasped object classification, human interaction classification, or learning-based control.

## 9 CONCLUSION

We have presented a method for rapidly digitally fabricating sensing-integrated pneumatic actuators *via* machine knitting. By programming our actuators at the stitch level, we can elicit desired deformation behavior. Resistive pressure sensors and swept frequency capacitive sensing electrodes can be integrated through conductive yarns while remaining resilient to the effects of large actuation. We offer a design interface for users to interactively program and preview the bending of actuators and the positions of the integrated sensors. We evaluate the usability and effectiveness of our design pipeline, reliability of our actuation, and capability of our sensing component. We demonstrate the application of our design tool to assistive wearables and soft robotics. We are excited to see our methodology deployed in other application domains in the future.

## ACKNOWLEDGMENTS

We thank Tao Du and Wan Shou for insightful discussions. We thank Roger White and Mieke Moran for the administration of the project. We thank the anonymous reviewers for their insightful comments.

## REFERENCES

- [1] Sean Ahlquist, Wes McGee, and Shahida Sharmin. 2017. PneumaKnit: Actuated architectures through wale-and course-wise tubular knit-constrained pneumatic systems. In *ACADIA*. CUMINCAD, Cambridge, MA, USA, 38–51.
- [2] Roland Aigner, Andreas Pointner, Thomas Preindl, Patrick Parzer, and Michael Haller. 2020. Embroidered Resistive Pressure Sensors: A Novel Approach for Textile Interfaces. In *Proceedings of the 2020 CHI Conference on Human Factors in Computing Systems* (Honolulu, HI, USA) (*CHI '20*). Association for Computing Machinery, New York, NY, USA, 1–13.
- [3] Lea Albaugh, Scott Hudson, and Lining Yao. 2019. Digital Fabrication of Soft Actuated Objects by Machine Knitting. In *Proceedings of the 2019 CHI Conference on Human Factors in Computing Systems* (Glasgow, Scotland Uk) (*CHI '19*). Association for Computing Machinery, New York, NY, USA, 1–13.
- [4] Ernar Amanov, Thien-Dang Nguyen, and Jessica Burgner-Kahrs. 2021. Tendon-driven continuum robots with extensible sections—A model-based evaluation of path-following motions. *The International Journal of Robotics Research* 40, 1 (2021), 7–23.
- [5] Alan T Asbeck, Stefano MM De Rossi, Ignacio Galiana, Ye Ding, and Conor J Walsh. 2014. Stronger, smarter, softer: next-generation wearable robots. *IEEE Robotics & Automation Magazine* 21, 4 (2014), 22–33.
- [6] Moritz Bächer, Benjamin Hepp, Fabrizio Pece, Paul G. Kry, Bernd Bickel, Bernhard Thomaszewski, and Otmar Hilliges. 2016. DefSense: Computational Design of Customized Deformable Input Devices. In *Proceedings of the 2016 CHI Conference on Human Factors in Computing Systems* (San Jose, California, USA) (*CHI '16*). Association for Computing Machinery, New York, NY, USA, 3806–3816.
- [7] Yuliya Baranovskaya, Marshall Prado, Moritz Dörstelmann, and Achim Menges. 2016. Knitflatable Architecture-Pneumatically Activated Preprogrammed Knit-Texiles. In *Proceedings of the 34th eCAADe Conference*. CUMINCAD, Oulu, Finland, 571–580.
- [8] Nicholas W Bartlett, Michael T Tolley, Johannes TB Overvelde, James C Weaver, Bobak Mosadegh, Katia Bertoldi, George M Whitesides, and Robert J Wood. 2015. A 3D-printed, functionally graded soft robot powered by combustion. *Science* 349, 6244 (2015), 161–165.
- [9] James M Bern, Kai-Hung Chang, and Stelian Coros. 2017. Interactive design of animated plushies. *ACM Transactions on Graphics (TOG)* 36, 4 (2017), 1–11.
- [10] Sofien Bouaziz, Mario Deuss, Yuli Schwartzburg, Thibaut Weise, and Mark Pauly. 2012. Shape-Up: Shaping Discrete Geometry with Projections. *Comput. Graph. Forum* 31, 5 (Aug. 2012), 1657–1667.
- [11] Sofien Bouaziz, Sébastien Martin, Tiantian Liu, Ladislav Kavan, and Mark Pauly. 2014. Projective Dynamics: Fusing Constraint Projections for Fast Simulation. *ACM Trans. Graph.* 33, 4, Article 154 (July 2014), 11 pages.
- [12] Leonardo Cappello, Kevin C Galloway, Siddharth Sanan, Diana A Wagner, Rachael Granberry, Sven Engelhardt, Florian L Haufe, Jeffrey D Peisner, and Conor J Walsh. 2018. Exploiting textile mechanical anisotropy for fabric-based pneumatic actuators. *Soft robotics* 5, 5 (2018), 662–674.
- [13] Alex Chortos, Ehsan Hajiesmaili, Javier Morales, David R Clarke, and Jennifer A Lewis. 2020. 3D printing of interdigitated dielectric elastomer actuators. *Advanced Functional Materials* 30, 1 (2020), 1907375.
- [14] Ching-Ping Chou and Blake Hannaford. 1996. Measurement and modeling of McKibben pneumatic artificial muscles. *IEEE Transactions on robotics and automation* 12, 1 (1996), 90–102.
- [15] Dylan Drotman, Michael Ishida, Saurabh Jadhav, and Michael T Tolley. 2018. Application-driven design of soft, 3-D printed, pneumatic actuators with bellows. *IEEE/ASME Transactions on Mechatronics* 24, 1 (2018), 78–87.
- [16] Tao Du, Kui Wu, Pingchuan Ma, Sébastien Wah, Andrew Spielberg, Daniela Rus, and Wojciech Matusik. 2021. DiffPD: Differentiable Projective Dynamics. *ACM Trans. Graph.* 41, 2, Article 13 (Nov 2021), 21 pages.
- [17] Hend M Elmoughni, Ayse Feyza Yilmaz, Kadir Ozlem, Fidan Khalilbayli, Leonardo Cappello, Asli Tunçay Atalay, Gökhân İnce, and Özgür Atalay. 2021. Machine-Knitted Seamless Pneumatic Actuators for Soft Robotics: Design, Fabrication, and Characterization. *Actuators* 10, 5 (2021), 94.
- [18] Qi Ge, Amir Hosein Sakhai, Howon Lee, Conner K Dunn, Nicholas X Fang, and Martin L Dunn. 2016. Multimaterial 4D printing with tailororable shape memory polymers. *Scientific reports* 6, 1 (2016), 1–11.
- [19] Jun Gong, Yu Wu, Lei Yan, Teddy Seyed, and Xing-Dong Yang. 2019. Tessutivo: Contextual Interactions on Interactive Fabrics with Inductive Sensing. In *Proceedings of the 32nd Annual ACM Symposium on User Interface Software and Technology* (New Orleans, LA, USA) (*UIST '19*). Association for Computing Machinery, New York, NY, USA, 29–41.
- [20] Min-Woo Han and Sung-Hoon Ahn. 2017. Blooming knit flowers: Loop-linked soft morphing structures for soft robotics. *Advanced materials* 29, 13 (2017), 1606580.
- [21] Bianca S Homberg, Robert K Katschmann, Mehmet R Dogar, and Daniela Rus. 2015. Haptic identification of objects using a modular soft robotic gripper. In *2015 IEEE/RSJ International Conference on Intelligent Robots and Systems (IROS)*. IEEE, New York, NY, USA, 1698–1705.
- [22] Colin Honigman, Jordan Hochenbaum, and Ajay Kapur. 2014. Techniques in Swept Frequency Capacitive Sensing: An Open Source Approach.. In *Proceedings of the International Conference on New Interfaces for Musical Expression*. NIME, London, United Kingdom, 74–77.
- [23] Yuanming Hu, Jiancheng Liu, Andrew Spielberg, Joshua B Tenenbaum, William T Freeman, Jiajun Wu, Daniela Rus, and Wojciech Matusik. 2019. Chainqueen: A real-time differentiable physical simulator for soft robotics. In *2019 International conference on robotics and automation (ICRA)*. IEEE, ACM New York, NY, USA, 6265–6271.
- [24] Scott E. Hudson. 2014. Printing Teddy Bears: A Technique for 3D Printing of Soft Interactive Objects. In *Proceedings of the SIGCHI Conference on Human Factors in Computing Systems* (Toronto, Ontario, Canada) (*CHI '14*). Association for Computing Machinery, New York, NY, USA, 459–468.
- [25] Josie Hughes, Andrew Spielberg, Mark Chounlakone, Gloria Chang, Wojciech Matusik, and Daniela Rus. 2020. A Simple, Inexpensive, Wearable Glove with Hybrid Resistive-Pressure Sensors for Computational Sensing, Proprioception, and Task Identification. *Advanced Intelligent Systems* 2, 6 (2020), 2000002.
- [26] Bong-Soo Kang, Curt S Kothera, Benjamin KS Woods, and Norman M Wereley. 2009. Dynamic modeling of McKibben pneumatic artificial muscles for antagonistic actuation. In *2009 IEEE International Conference on Robotics and Automation*. IEEE, New York, NY, USA, 182–187.
- [27] Mehmet Kanik, Sırma Orguc, Georgios Varnavides, Jinwoo Kim, Thomas Benavides, Dani Gonzalez, Timothy Akintilo, C Cem Tasan, Anantha P Chandrakasan, Yoel Fink, et al. 2019. Strain-programmable fiber-based artificial muscle. *Science* 365, 6449 (2019), 145–150.

- [28] Alexandre Kaspar, Liane Makatura, and Wojciech Matusik. 2019. Knitting Skeletons: A Computer-Aided Design Tool for Shaping and Patterning of Knitted Garments. In *Proceedings of the 32nd Annual ACM Symposium on User Interface Software and Technology* (New Orleans, LA, USA) (*UIST '19*). Association for Computing Machinery, New York, NY, USA, 53–65.
- [29] Alexandre Kaspar, Kui Wu, Yiyue Luo, Liane Makatura, and Wojciech Matusik. 2021. Knit Sketching: From Cut & Sew Patterns to Machine-Knit Garments. *ACM Trans. Graph.* 40, 4, Article 63 (jul 2021), 15 pages.
- [30] Ozgur Kilic Afşar, Ali Shtarbanov, Hila Mor, Ken Nakagaki, Jack Forman, Karen Modrei, Seung Hee Jeong, Klas Hjort, Kristina Höök, and Hiroshi Ishii. 2021. OmniFiber: Integrated Fluidic Fiber Actuators for Weaving Movement Based Interactions into the ‘Fabric of Everyday Life’. In *The 34th Annual ACM Symposium on User Interface Software and Technology* (Virtual Event, USA) (*UIST '21*). Association for Computing Machinery, New York, NY, USA, 1010–1026.
- [31] Arda Kotikian, Javier M Morales, Aric Lu, Jochen Mueller, Zoey S Davidson, J William Boley, and Jennifer A Lewis. 2021. Innervated, Self-Sensing Liquid Crystal Elastomer Actuators with Closed Loop Control. *Advanced Materials* 33 (2021), 2101814.
- [32] Yiyue Luo, Yunzhu Li, Pratyusha Sharma, Wan Shou, Kui Wu, Michael Foshey, Beichen Li, Tomás Palacios, Antonio Torralba, and Wojciech Matusik. 2021. Learning human–environment interactions using conformal tactile textiles. *Nature Electronics* 4, 3 (2021), 193–201.
- [33] Yiyue Luo, Kui Wu, Tomás Palacios, and Wojciech Matusik. 2021. KnitUI: Fabricating Interactive and Sensing Textiles with Machine Knitting. In *Proceedings of the 2021 CHI Conference on Human Factors in Computing Systems* (Yokohama, Japan) (*CHI '21*). Association for Computing Machinery, New York, NY, USA, Article 668, 12 pages.
- [34] Li-Ke Ma, Yizhong Zhang, Yang Liu, Kun Zhou, and Xin Tong. 2017. Computational design and fabrication of soft pneumatic objects with desired deformations. *ACM Transactions on Graphics (TOG)* 36, 6 (2017), 1–12.
- [35] Robert MacCurdy, Robert Katzschnmann, Youbin Kim, and Daniela Rus. 2016. Printable hydraulics: A method for fabricating robots by 3D co-printing solids and liquids. In *2016 IEEE International Conference on Robotics and Automation (ICRA)*. IEEE, New York, NY, USA, 3878–3885.
- [36] Andrew D Marchese, Robert K Katzschnmann, and Daniela Rus. 2015. A recipe for soft fluidic elastomer robots. *Soft robotics* 2, 1 (2015), 7–25.
- [37] James McCann. 2017. The “Knitout” (.k) File Format. [Online]. Available from: <https://textiles-lab.github.io/knitout/knitout.html>.
- [38] James McCann, Lea Albaugh, Vidya Narayanan, April Grow, Wojciech Matusik, Jennifer Mankoff, and Jessica Hodgins. 2016. A compiler for 3D machine knitting. *ACM Transactions on Graphics (TOG)* 35, 4 (2016), 1–11.
- [39] David McCoul, Samuel Rosset, Samuel Schlatter, and Herbert Shea. 2017. Inkjet 3D printing of UV and thermal cure silicone elastomers for dielectric elastomer actuators. *Smart Materials and Structures* 26, 12 (2017), 125022.
- [40] Aslan Miriyev, Kenneth Stack, and Hod Lipson. 2017. Soft material for soft actuators. *Nature communications* 8, 1 (2017), 1–8.
- [41] Vidya Narayanan, Kui Wu, Cem Yuksel, and James McCann. 2019. Visual knitting machine programming. *ACM Transactions on Graphics (TOG)* 38, 4 (2019), 1–13.
- [42] Pham Huy Nguyen and Wenlong Zhang. 2020. Design and computational modeling of fabric soft pneumatic actuators for wearable assistive devices. *Scientific reports* 10, 1 (2020), 1–13.
- [43] Ciarrán T. O'Neill, Connor M. McCann, Cameron J. Hohimer, Katie Bertoldi, and Conor J. Walsh. 2022. Unfolding Textile-Based Pneumatic Actuators for Wearable Applications. *Soft Robotics* 9, 1 (2022), 163–172. PMID: 33481682.
- [44] Jifei Ou, Daniel Oran, Don Derek Haddad, Joseph Paradiso, and Hiroshi Ishii. 2019. SensorKnit: architecting textile sensors with machine knitting. *3D Printing and Additive Manufacturing* 6, 1 (2019), 1–11.
- [45] Yong-Lae Park, Bor-Rong Chen, and Robert J Wood. 2012. Design and fabrication of soft artificial skin using embedded microchannels and liquid conductors. *IEEE Sensors journal* 12, 8 (2012), 2711–2718.
- [46] Patrick Parzer, Florian Perteneder, Kathrin Probst, Christian Rendl, Joanne Leong, Sarah Schütz, Anita Vogl, Reinhard Schwödauer, Martin Kaltenbrunner, Siegfried Bauer, and Michael Haller. 2018. RESi: A Highly Flexible, Pressure-Sensitive, Imperceptible Textile Interface Based on Resistive Yarns. In *UIST2018: Proceedings of the 31th Annual Symposium on User Interface Software and Technology*. ACM, Berlin, Germany, 745–756. [http://mi-lab.org/wp-content/uploads/2019/12/RESi\\_final.pdf](http://mi-lab.org/wp-content/uploads/2019/12/RESi_final.pdf)
- [47] Munehiko Sato, Ivan Poupyrev, and Chris Harrison. 2012. Touché: Enhancing Touch Interaction on Humans, Screens, Liquids, and Everyday Objects. In *Proceedings of the SIGCHI Conference on Human Factors in Computing Systems* (Austin, Texas, USA) (*CHI '12*). Association for Computing Machinery, New York, NY, USA, 483–492.
- [48] Sangok Seok, Cagdas Denizel Onal, Kyu-Jin Cho, Robert J Wood, Daniela Rus, and Sangbae Kim. 2012. Meshworm: a peristaltic soft robot with antagonistic nickel titanium coil actuators. *IEEE/ASME Transactions on mechatronics* 18, 5 (2012), 1485–1497.
- [49] Gaurav Singh and Girish Krishnan. 2017. A constrained maximization formulation to analyze deformation of fiber reinforced elastomeric actuators. *Smart Materials and Structures* 26, 6 (2017), 065024.
- [50] Mélina Skouras, Bernhard Thomaszewski, Peter Kaufmann, Akash Garg, Bernd Bickel, Eitan Grinspun, and Markus Gross. 2014. Designing Inflatable Structures. *ACM Trans. Graph.* 33, 4, Article 63 (July 2014), 10 pages.
- [51] Luca Somm, David Hahn, Nitish Kumar, and Stelian Coros. 2019. Expanding foam as the material for fabrication, prototyping and experimental assessment of low-cost soft robots with embedded sensing. *IEEE Robotics and Automation Letters* 4, 2 (2019), 761–768.
- [52] Javier Tapia, Espen Knoop, Mojmir Mutný, Miguel A Otaduy, and Moritz Bächer. 2020. Makesense: Automated sensor design for proprioceptive soft robots. *Soft robotics* 7, 3 (2020), 332–345.
- [53] Thomas George Thuruthel, Benjamin Shih, Cecilia Laschi, and Michael Thomas Tolley. 2019. Soft robot perception using embedded soft sensors and recurrent neural networks. *Science Robotics* 4, 26 (2019), eaav1488.
- [54] Calleit Votzke, Urانбилек Даалхайяв, Yiğit Mengüç, and Matthew L Johnston. 2019. 3D-printed liquid metal interconnects for stretchable electronics. *IEEE Sensors Journal* 19, 10 (2019), 3832–3840.
- [55] Michael Wehner, Ryan L Truby, Daniel J Fitzgerald, Bobak Mosadegh, George M Whitesides, Jennifer A Lewis, and Robert J Wood. 2016. An integrated design and fabrication strategy for entirely soft, autonomous robots. *Nature* 536, 7617 (2016), 451–455.
- [56] Kui Wu, Xifeng Gao, Zachary Ferguson, Daniele Panozzo, and Cem Yuksel. 2018. Stitch Meshing. *ACM Trans. Graph. (Proceedings of SIGGRAPH 2018)* 37, 4, Article 130 (jul 2018), 14 pages.
- [57] Kui Wu, Hannah Swan, and Cem Yuksel. 2019. Knittable Stitch Meshes. *ACM Trans. Graph.* 38, 1, Article 10 (Jan. 2019), 13 pages.
- [58] Kui Wu, Marco Tarini, Cem Yuksel, Jim McCann, and Xifeng Gao. 2021. Wearable 3D Machine Knitting: Automatic Generation of Shaped Knit Sheets to Cover Real-World Objects. *IEEE Transactions on Visualization & Computer Graphics* 1, 01 (feb 2021), 1–1.
- [59] Lianjun Wu, Indrajeet Chauhan, and Yonas Tadesse. 2018. A novel soft actuator for the musculoskeletal system. *Advanced Materials Technologies* 3, 5 (2018), 1700359.
- [60] Te-Yen Wu, Lu Tan, Yuji Zhang, Teddy Seyed, and Xing-Dong Yang. 2020. Capacitivo: Contact-Based Object Recognition on Interactive Fabrics Using Capacitive Sensing. Association for Computing Machinery, New York, NY, USA, 649–661.
- [61] Hong Kai Yap, Phone May Khin, Tze Hui Koh, Yi Sun, Xinquan Liang, Jeong Hoon Lim, and Chen-Hua Yeow. 2017. A fully fabric-based bidirectional soft robotic glove for assistance and rehabilitation of hand impaired patients. *IEEE Robotics and Automation Letters* 2, 3 (2017), 1383–1390.
- [62] Michael C Yip and Günter Niemeyer. 2015. High-performance robotic muscles from conductive nylon sewing thread. In *2015 IEEE International Conference on Robotics and Automation (ICRA)*. IEEE, New York, NY, USA, 2313–2318.
- [63] Osman Dogan Yirmibesoglu, John Morrow, Steph Walker, Walker Gosrich, Reece Cañizares, Hansung Kim, Urانбилек Даалхайяв, Chloe Fleming, Callie Branyan, and Yiğit Mengüç. 2018. Direct 3D printing of silicone elastomer soft robots and their performance comparison with molded counterparts. In *2018 IEEE International Conference on Soft Robotics (RoboSoft)*. IEEE, New York, NY, USA, 295–302.
- [64] Tianhong Catherine Yu and James McCann. 2020. Coupling Programs and Visualization for Machine Knitting. In *Symposium on Computational Fabrication (Virtual Event, USA) (SCF '20)*. Association for Computing Machinery, New York, NY, USA, Article 7, 10 pages.
- [65] Cem Yuksel, Jonathan M. Kaldor, Doug L. James, and Steve Marschner. 2012. Stitch Meshes for Modeling Knitted Clothing with Yarn-level Detail. *ACM Trans. Graph. (Proceedings of SIGGRAPH 2012)* 31, 3, Article 37 (2012), 12 pages.